Journal of Power Sources 235 (2013) 181–186

Contents lists available at SciVerse ScienceDirect

Journal of Power Sources

journal homepage: www.elsevier.com/locate/jpowsour

Shuttle phenomenon – The irreversible oxidation mechanism of sulfur active material in Li–S battery

Yan Diao*, Kai Xie, Shizhao Xiong, Xiaobin Hong

College of Aerospace Science and Engineering, National University of Defense Technology, Changsha 410073, China

HIGHLIGHTS

- The Li–S batteries solvent degradation products is the oxygen source of the sulfur active material irreversible oxidation.
- The shuttle phenomenon is an important reason leading to the active material irreversible oxidation.
- The overcharging capacity of Li–S batteries consists of a reversible part and an irreversible part.
- The long-chain lithium polysulfide oxidized to Li_xSO_y species leads to the irreversible overcharging capacity.

ARTICLE INFO

Article history:
Received 18 November 2012
Received in revised form
17 January 2013
Accepted 19 January 2013
Available online 31 January 2013

Keywords:
Lithium–sulfur battery
Sulfur cathode
Capacity fading
Sulfur active material irreversible oxidation

ABSTRACT

The commercialization of lithium–sulfur batteries is hindered by serious capacity fading that mainly results from the irreversible oxidation of sulfur active material during cycling, but so far the underlying oxidation mechanism still remains unclear. The research results reveal that the most practical solvent DOL and DME are not stable and large amount of degradation products with -OLi edge groups become the oxygen source. The shuttle phenomenon is an important reason leading to the irreversible oxidation of sulfur active material, which results from series chemical reductions of lithium polysulfide, and they keep charge conservation by their selves, but prolong the charge process and lead to the overcharging. In charge process, the low speed reactions of long-chain lithium polysulfide oxidized to Li_xSO_y species exist in the electrolyte, which are indistinctly in the systems without overcharging. As the shuttle phenomenon prolongs the charge process, the irreversible oxidation reactions become distinctly, and the Li_xSO_y species are detectable. The overcharging capacity could be explained as a reversible part and an irreversible part. The reversible capacity is from the cathode active material oxidized to long-chain lithium polysulfide and elemental sulfur, and the irreversible capacity is from the long-chain lithium polysulfide oxidized to Li_xSO_y species.

1. Introduction

Rechargeable Li–S battery possesses more advantages over the conventional lithium ion battery, but the practical use faces with serious capacity fading and poor cycle performance [1,2]. During the last three decades, capacity fading mechanisms of Li–S battery have been studied extensively. Firstly, lithium anode reacts with electrolyte solvent, such as dioxolane (DOL), dimethoxyethane (DME) producing ROLi and HCO_2Li, and the solvent is consumed with cycling until depletion [3]. Secondly, a peculiar problem in Li–S battery is the shuttle phenomenon. The discharge product, long-chain lithium polysulfide dissolving in electrolyte diffuses to the lithium anode where they react directly with the lithium in a parasitic reaction to produce the lower-order polysulfide. These species diffuse back to the sulfur cathode to generate the higher forms of polysulfide again, thus a shuttle mechanism is created. The shuttle phenomenon not only induces lithium corrosion, but also results in the self-discharge and the low coulomb efficiency [4–6]. Thirdly, high ordered lithium polysulfide (Li_2S_n, $3 \leq n \leq 8$) is soluble in electrolyte, but low ordered lithium polysulfide (Li_2S_2 and Li_2S) is insoluble. Thus chemical precipitation/dissolution reactions occur during the electrochemical process resulting in active material transition between liquid phase and solid phase. But it is difficult for the high ordered lithium polysulfide to transfer completely from liquid phase to solid phase at the end of cycles, so that will lead to the active material loss. [7] Fourthly, researchers impute the capacity fading into the residual Li_2S_2 and Li_2S in sulfur cathode even at 100% depth of charge. The formation of Li_2S_2 and Li_2S increasing

* Corresponding author. Tel./fax: +86 731 84573149.
E-mail address: diaoyandiaoyan@sina.com (Y. Diao).

0378-7753/$ – see front matter © 2013 Elsevier B.V. All rights reserved.
http://dx.doi.org/10.1016/j.jpowsour.2013.01.132

with cycling results in active material loss. And the deposition of irreversible Li_2S or Li_2S_2 at cracked surfaces of carbon particles causes cathode structural failure [8–10].

In our previous researches [11], the irreversibility of Li_2S and Li_2S_2 are not serious as in reports. Electrolyte degradation products co-deposit with Li_2S and Li_2S_2 in discharge process, and accumulate in cathodes leading to the cathodes structural deterioration. Another serious problem is the irreversible oxidation of cathode active material. The formation of Li_xSO_y species increasing with cycling indicates an important capacity fading mechanism of Li–S battery. However, reasons leading to the active material oxidation need to be further researched.

In this work, we design a series of experiments to find out the factors resulting in sulfur active material oxidation. We synthesize Li_2S_n ($3 \leq n \leq 8$) firstly, as the intermediate products and sulfur active material, it can take the role of ions transfer after the discharge process beginning. Li_2S_n ($3 \leq n \leq 8$) selected as lithium salts to assemble Li–S cells can exclude the impact of lithium salts, and then we can make clear that whether the solvents could become the oxygen source. We assemble cells using 1 M Li_2S_n ($3 \leq n \leq 8$)/DOL/DME, 0.5 M $LiNO_3$/DOL/DME and 0.5 M LiTFSI/DOL/DME as electrolyte. Compared the results of different electrolyte system, we can identify the different reason leading to the sulfur active material oxidation. Fourier transform infrared (FTIR) is used to characterize the electrolyte solution. X-ray photoelectron spectroscopy (XPS) is used to confirm sulfur containing species in sulfurs. And liquid chromatography (LC) is used to test the change of lithium salts in electrolyte.

2. Experimental

2.1. The preparation of Li_2S_n ($3 \leq n \leq 8$)

Li_2S_n ($3 \leq n \leq 8$) was prepared by adding stoichiometric amounts of lithium (100 μm thick lithium foil, >99.9%, Denway, China) and sulfur (S_8, 99.5%, Aldrich) in DOL and DME solvent (1:1, V:V, Novolyte, China). The mixture was tightly capped and stirred vigorously for 72 h at room temperature in inert atmosphere [3,7]. It was impossible to obtain pure lithium polysulfide with mono chain length, which could be confirmed from the LC graph shown in Fig. 6. The concentration of Li_2S_n ($3 \leq n \leq 8$) calculated by the concentration of sulfur was about 1 M.

2.2. Preparation of Li–S cells

The sulfur cathode materials consisted of 52 wt % sulfur, 35wt % Super-P carbon, and 13wt% poly (vinylidene fluoride) binder. The cathode materials were slurry-cast onto a carbon-coated aluminum current collector with typical active material loading of 1.0 mg cm^{-2}. The electrodes were dried under vacuum at 50 °C for 12 h. The cells were assembled in an argon-filled glove box (MIKROUNA, China) using lithium foil as anode and a porous polyolefin separator (Celgard®2500, USA). About 0.04 mL electrolyte per milligram sulfur was sealed with other parts of the cells in an aluminum coated plastic pack under vacuum. The electrolyte was choose from 1M Li_2S_n ($3 \leq n \leq 8$)/DOL/DME, 0.5 M $LiNO_3$/DOL/DME and 0.5 M LiTFSI/DOL/DME.

2.3. The electrochemical measurement

Discharge-charge performances of the cells at the current density of 0.168 mA cm^{-2} were tested on a multi-channel battery tester (LAND CT2001A). All the tests were carried out at room temperature.

2.4. Preparation of characteristic samples

The Li_2S_n ($3 \leq n \leq 8$) solution coated on KBr pallet was used for FTIR measurement. The solution was also coated on slides, and then the lithium salt was deposited on the slide after the solvent evaporation in argon-filled glove box. The slide coated with lithium polysulfide was used for XPS measurement.

In order to study the condition of active material in Li–S cells, the cells were disassembled in argon-filled glove box. The sulfur cathode, lithium anode, separator and the package were washed by DOL respectively. The collected solution containing electrochemical products was diluted to 25 mL by DOL. Then 1 mL the solution was diluted to 100 times by DOL solvent for the LC measurement. The sulfur cathodes were separated and rinsed several times with pure DOL to remove electrolyte residue. Pieces of cathodes used for XPS measurement were all placed in an inert atmosphere during sample preparation.

2.5. Characterization of samples

Transmission spectra of FITR were obtained on a Nicolet 6700 spectrometer. For the LC measurement, about 10 μL sample was injected into LC instrument (Tianmei-2000) after filtrated, and then was eluted on a reverse phase C18 column (250 mm × 4.6 mm), detected by a UV detector. The flow rate of methanol as elution phase was 1 mL min^{-1}. Absorbance was measured at 210 nm. The samples used for XPS measurements were carried out at a K-Alpha 1063(Thermo Fisher Scientific) spectrometer. Monochromatic Al-Kα was used as excitation. The typical analysis area is 400 μm in diameter and the pressure for the analysis chamber is 10^{-9} mbar. Binding energy scale was corrected based on C_{1s} peak from contaminations (around 284.8 eV) as the internal binding energy standard. The Shirley background, the mixed Gaussian/Lorentzian approach, was used for the fitting of the high resolution S_{2p} peaks by the software (Thermo Avantage).

3. Results and discussion

3.1. Effects of shuttle phenomenon on the irreversible oxidation of sulfur active material

1 M Li_2S_n ($3 \leq n \leq 8$) electrolyte solution was prepared, and the FTIR spectra compared with DOL and DME was shown in Fig. 1. Peak assignments for the FTIR obtained in these studies were marked near the main peaks. Peak at 935 cm^{-1} was the ring vibration of DOL [12], but in Li_2S_n ($3 \leq n \leq 8$) solution the ring vibration peak almost disappeared, which indicated the ring-opening reaction of DOL. The characteristic peaks at 1002 cm^{-1} and 1124 cm^{-1} were related to the C–O band stretching vibration due to DOL, DME and ROLi species [3,11,12]. In the spectra of Li_2S_n ($3 \leq n \leq 8$) solution, the peaks at 1640 cm^{-1} and 1428 cm^{-1} reflected the COO^- band stretching vibration due to the formation of HCO_2Li [3,12,13]. Peak at 870 cm^{-1} was related to the Li–O bending vibration reflected the formation of ROLi, HCO_2Li, and poly-DOL oligomers with -OLi edge groups [11]. All of these products had been detected as the surface components of Li electrode and the electrolyte degradation products in Li–S cells [11], and the main reaction schemes had been described by Aurbach et al. [3] and Mikhaylik et al. [6] in details. These products suggested that DOL and DME solvent were not stable and the solvent degradation was inevitable in Li–S system.

We assembled Li–S cells with 1 M Li_2S_n ($3 \leq n \leq 8$)/DOL/DME as electrolyte, and the discharge–charge profiles were displayed in Fig. 2. The cells were disassembled after discharging to 1.7 V, charging to 2.35 V and shuttling at 2.35 V about 16 h. Then the sulfur cathodes were used for XPS measurement to confirm the products.

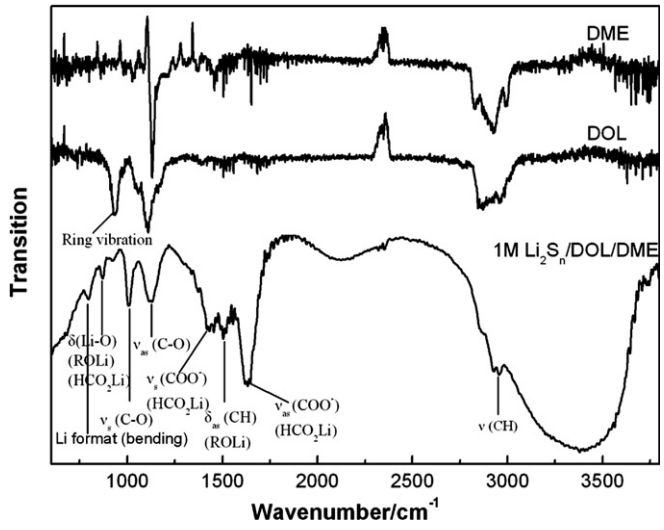

Fig. 1. FTIR spectrum of Li_2S_n solution.

Fig. 3 showed S_{2p} spectrum of sulfur cathodes after cycling. In XPS measurement, sulfur element always had two characteristic peaks, and the superposition of deconvoluted peaks made the identification of sulfur containing species obscurely. But basing on the principle of XPS measurement, the higher banding energy corresponded to higher oxidation state. In S_{2p} spectrum of Li_2S_n ($3 \leq n \leq 8$), peak at 162.9 eV was assigned to Li–S band [3,14,15], and peak at 164.0 eV was assigned to S–S band [16,17]. After the cells discharged to 1.7 V, the prominent broad S_{2p} peaks around 160–162 eV were deconvoluted into two sharper peaks at 160.0 and 161.5 eV, which could be assigned to Li–S band from Li_2S_2 and Li_2S deposited in sulfur cathode [3,14]. Peaks at 162.9 eV and 164.0 eV were also corresponding to Li–S band and S–S band from Li_2S_n. After the cells charged to 2.35 V, peaks located at 164.0 eV and 165.3 eV were the characteristic peaks of S_8 [16,17], which was a direct evidence of the formation of S_8 in cathodes. After the cells shuttling at 2.35 V about 16 h, besides the peaks from S_8, large amount of S–O band located at banding energy higher than 166.0 eV were formed, and it indicated the formation of Li_xSO_y [3,11,14,15,18–20]. In Fig. 3c and d, few peaks lower than 162.0 eV were found indicating the good reversibility of Li_2S_2 and Li_2S.

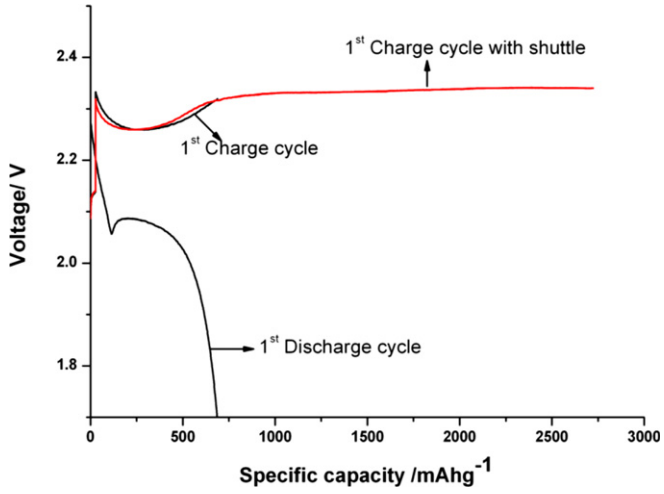

Fig. 2. Discharge–charge curves of Li–S cells with 1 M Li_2S_n/DOL/DME electrolyte.

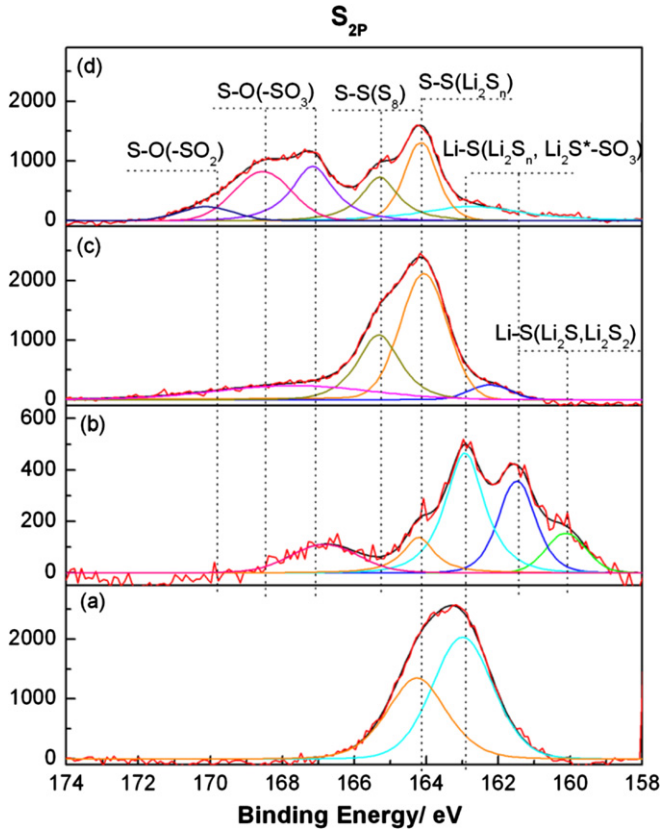

Fig. 3. S_{2p} spectrum of cathodes cycling with 1 M Li_2S_n/DOL/DME electrolyte. (a) 1 M Li_2S_n/DOL/DME electrolyte, (b) The 1st discharge cycle, (c) The 1st charge cycle, (d) The 1st charge cycle with shuttle phenomenon.

The formation of sulfur oxidation species Li_xSO_y in Fig. 3d could be explained as follow. Firstly, because the DOL and DME solvent were not stable, large amount of solvent degradation products with -OLi edge groups could become the oxygen source of the Li_xSO_y species formation. Secondly, the shuttle phenomenon enhanced the active material irreversible oxidation. The shuttle phenomenon could protect Li–S cells to avoid the harmful overcharging, but the overcharging of cells could result in the coulomb efficiency degradation [5]. In charge process, the electrons transferred from the cathode active materials to the electrode until the charging cut off voltage. In the common used lithium salts electrolyte system of Li–S cells, such as LiTFSI, $LiClO_4$, $LiNO_3$, the charging cut off voltage were always higher than 2.4 V. However, in Li_2S_n ($3 \leq n \leq 8$) electrolyte system, because of the high concentration of lithium polysulfide, the shuttle phenomenon was enhanced, and the charging voltage maintained at 2.32 V–2.35 V. When S_n^{2-} contacted the solvent degradation products with -OLi edge groups and had to give out electrons continually, the Li_xSO_y was formed which could be described in Scheme 1.

To identify the effects of shuttle phenomenon on the cycle performance, we assembled cells with 1 M Li_2S_n ($3 \leq n \leq 8$)/DOL/DME and 0.5 M LiTFSI/DOL/DME. The cycle performances of the cells were shown in Fig. 4. After 20 discharge cycles, the cells were disassembled, and the sulfur cathodes were separated for XPS measurement to confirm the sulfur compounds shown in Fig. 5. The

$$\text{-OLi} + S_n^{2-} \text{-e} \rightarrow Li_xSO_y + S_{n-1}^{2-} \quad (1)$$

Scheme 1.

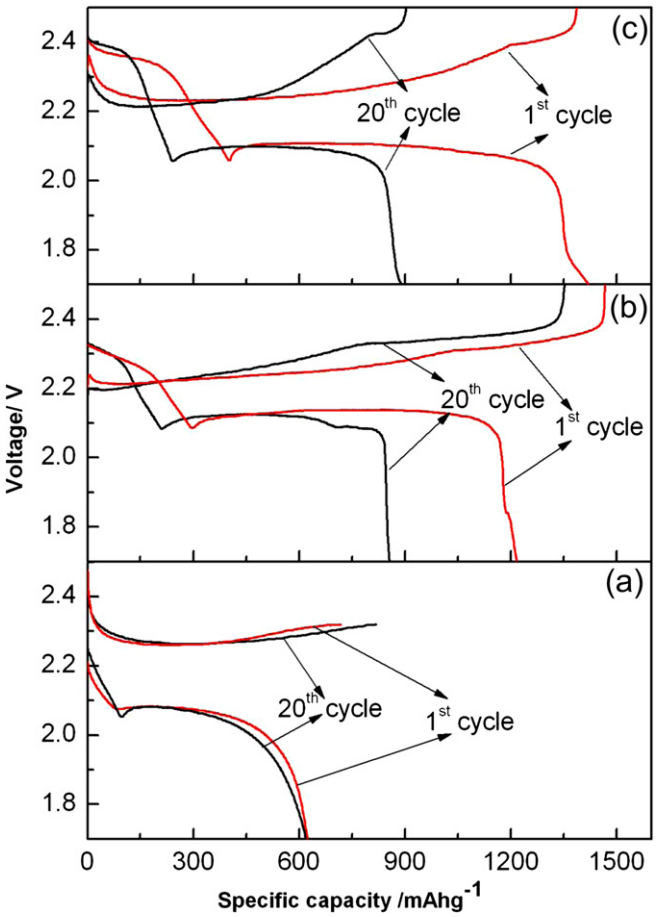

Fig. 4. Cycle performances of Li–S cells with different electrolyte solution after 20 cycles. (a) 1 M Li_2S_n/DOL/DME, (b) 0.5 M LiTFSI/DOL/DME, (c) 0.5 M $LiNO_3$/DOL/DME.

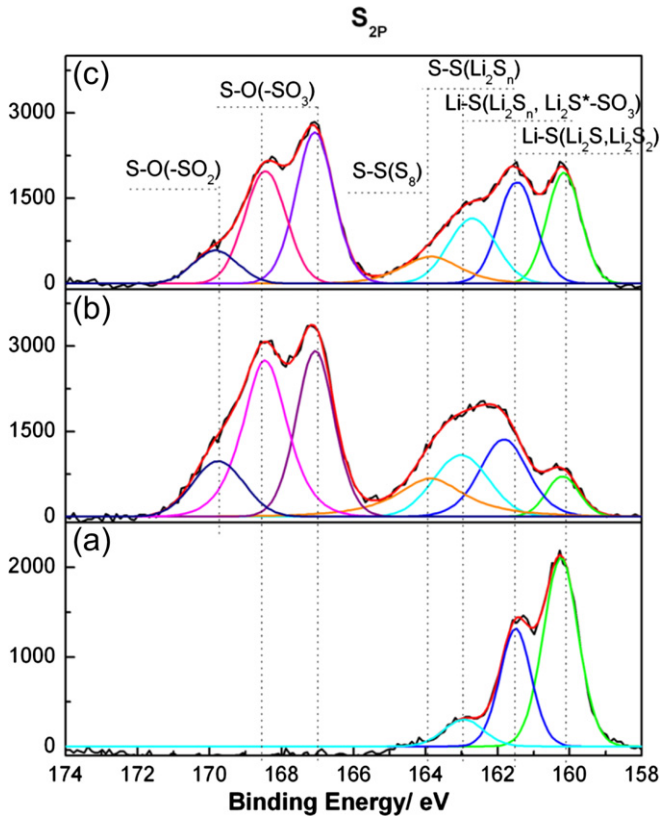

Fig. 5. S_{2p} spectrum of cathodes after 20 discharge cycles (a) 1 M Li_2S_n/DOL/DME, (b) 0.5 M LiTFSI/DOL/DME, (c) 0.5 M $LiNO_3$/DOL/DME.

rinse solution containing electrochemical products was used for LC measurement shown in Fig. 6.

In order to alleviate the impact of the shuttle phenomenon, the charging cut off voltage of cells cycling with Li_2S_n ($3 \leq n \leq 8$) electrolyte was controlled at 2.32 V shown in Fig. 4a. In discharge cycle, the high discharge plateau was short, and the discharge capacity was mainly from the low discharge plateau which corresponding to the process of long-chain lithium polysulfide transferring to low-ordered lithium polysulfide (Li_2S and Li_2S_2) [7]. The discharge capacity was just 624 mAh g^{-1}. In Fig. 5a, after 20 cycles few Li_xSO_y species was formed in Li_2S_n ($3 \leq n \leq 8$) system. It indicated that if the shuttle phenomenon was controlled, the sulfur active material irreversible oxidation could be alleviated. In Fig. 6, peak at 2.3838 min was from Li_2S_4, and peak at 5.8084 min was from Li_2S_6. The LC spectrum of Li_2S_n ($3 \leq n \leq 8$) solution suggested that pure lithium polysulfide with mono chain length was unobtainable, and Li_2S_4 and Li_2S_6 were the most stable form of lithium polysulfide species in Li–S system [7].

In LiTFSI system, another form of the shuttle phenomenon was revealed. The charging cut off voltage of cells could be increased to 2.5 V, but the coulomb efficiency was low, and the overcharging was serious. The discharge capacity shown in Fig. 4b degraded from 1217 mAh g^{-1} to 856 mAh g^{-1} in 20 cycles. After 20 cycles, in Fig. 5b the abundant S–O band locating at banding energy higher than 166.0 eV indicated the formation of Li_xSO_y species in cathode. In Fig. 6, peak at 1.6999 min was from LiTFSI salt, and after 20 cycles this peak was almost the same as the LiTFSI electrolyte. It showed that the LiTFSI salt was stable in Li–S system with cycling, and the formation of Li_xSO_y species was mostly from the sulfur active material irreversible oxidation. But the oxidation mechanism of the sulfur active material in LiTFSI system was indistinct. We could obtain some meaningful information from the low coulomb efficiency (63.3%) in the 20th cycle. The charge capacity as 1.58 times as the discharge capacity indicated that the shuttle phenomenon was active in LiTFSI system.

The shuttle phenomenon was resulted from series chemical equilibrium reactions [4]: the long-chain lithium polysulfide dissolved in the electrolyte reacted with metallic lithium on anode (reactions (1) and (2)); the long-chain lithium polysulfide reacted with insoluble Li_2S_2 and Li_2S on cathode (reactions (3) and (4)).

$$2Li + Li_2S_n \rightarrow Li_2S\downarrow + Li_2S_{n-1} \quad (1)$$

$$2Li + Li_2S_n \rightarrow Li_2S_2\downarrow + Li_2S_{n-1} \quad (2)$$

$$Li_2S + Li_2S_n \rightarrow Li_2S_k + Li_2S_{n-k+1} \quad (3)$$

$$Li_2S_2 + Li_2Sn \rightarrow Li_2S_k + Li_2S_{n-k+2} \quad (4)$$

From the shuttle equations we could conclude that the transformation of long-chain lithium polysulfide and lower-order polysulfide in electrolyte was just related to the concentration of chemical equilibrium reactants, and these reactions kept charge conservation by their selves. In charge process, the cathode active material was oxidized to long-chain lithium polysulfide and

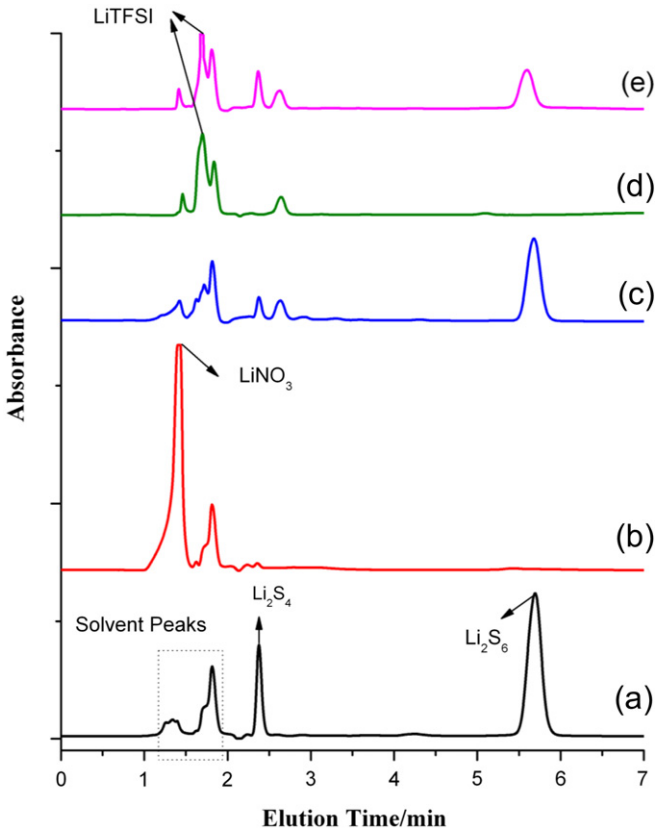

Fig. 6. LC spectrum of electrolyte solution eluted on a C18 column. (a) 1 M Li_2S_n/DOL/DME solution, (b) 0.5 M $LiNO_3$/DOL/DME solution, (c) $LiNO_3$ electrolyte solution after 20 cycles, (d) 0.5 M LiTFSI/DOL/DME, (e) LiTFSI electrolyte solution after 20 cycles.

elemental sulfur step by step [7], and then the high concentration of long-chain lithium polysulfide enhanced the shuttle phenomenon. The high plateau in the charging process would be an equilibrium state between electrochemical oxidation of the polysulfide and the chemical reduction of the polysulfide, resulting in the average oxidization level of the sulfur compounds. Thus, the active shuttle phenomenon prolonged the charge process and the overcharging happened.

At the same time, another kind of electrochemical oxidation, the long-chain lithium polysulfide oxidized to Li_xSO_y species also existed in the electrolyte, but the speeds of these reactions were very slow in electrochemical kinetics. And the reactions potential was close to the reactions of the cathode active material oxidized to long-chain lithium polysulfide and elemental sulfur, so it was difficult to identify the different oxidation peaks from the measurement of cyclic voltammetry (CV). As the shuttle phenomenon prolonged the charge process, the irreversible oxidation of the long-chain lithium polysulfide became distinctly, and the oxidation products Li_xSO_y were detectable. Thus, the overcharging capacity was suggested consisting of two parts: one part was from the reversible capacity of the cathode active material oxidized to long-chain lithium polysulfide and elemental sulfur; another part was from the irreversible capacity of the long-chain lithium polysulfide oxidized to Li_xSO_y species.

3.2. Effects of $LiNO_3$ — the shuttle phenomenon preventing additive on the irreversible oxidation of sulfur active material

The effects of shuttle phenomenon on the irreversible oxidation of sulfur active material had been discussed in details, and the

$$LiNO_3 + Li_2S_n \rightarrow Li_mNO_n + Li_xSO_y \qquad (2)$$

Scheme 2.

effects of $LiNO_3$, an well-known shuttle phenomenon preventing additive of Li–S cells [3], also should been paid more attention.

We assembled cells with 0.5 M $LiNO_3$/DOL/DME electrolyte. The cycle performance was shown in Fig. 4c. In 20 cycles, the discharge capacity degraded from 1422 mAh g^{-1} to 890 mAh g^{-1} in $LiNO_3$ electrolyte system, and the coulomb efficiency was 98.4% in the 20th cycle. The XPS spectra of cathode shown in Fig. 5c reflected the abundant Li_xSO_y species formation and the sulfur active material oxidation. The LC spectrum of the rinse solution containing electrochemical products was shown in Fig. 6. Peak at 1.4558 min was from $LiNO_3$ salt, which disappeared after 20 cycles, indicated the consumption of $LiNO_3$ [7].

Researchers have discussed and explained the positive effects of $LiNO_3$ on the surface film formation of lithium anode which contributed to the reaction between lithium metal and the electrolyte solution [3,21]. However, the compact and homogenous surface film could enhance the stability of lithium anode, and alleviate the shuttle phenomenon, but it still could not prevent the capacity degradation. In $LiNO_3$ electrolyte system, the coulomb efficiency higher than 98% indicated the shuttle phenomenon was controlled effectively. The irreversible oxidation of sulfur active material was still an important reason leading to the capacity fading, but the oxidation mechanism was different from the systems with active shuttle phenomenon. The $LiNO_3$ reacted with Li_2S_n in electrolyte could be described in Scheme 2, which was confirmed to be the main reaction on the lithium anode by Aurbach et al. [3]. From the results of XPS and LC, we supposed that the reactions not only occurred on the anode, but also in the whole system. The large amount of Li_xSO_y species formation on cathodes and the consumption of $LiNO_3$ in electrolyte reflected the negative effects of $LiNO_3$ on the irreversible oxidation of sulfur active material.

4. Conclusions

The most practical solvent DOL and DME of Li–S cells were not stable, and large amount of solvent degradation products with -OLi edge groups could become the oxygen source of the Li_xSO_y species formation. The shuttle phenomenon was an important reason leading to the irreversible oxidation of sulfur active material, which resulted from series chemical reductions of lithium polysulfide. Though the shuttle reactions kept charge conservation by their selves, but they prolonged the charge process and leaded to the overcharging. In charge process, the low speed reactions of long-chain lithium polysulfide oxidized to Li_xSO_y species were indistinctly in the systems without overcharging. As the shuttle phenomenon prolonged the charge process, the irreversible oxidation reactions became distinctly, and the Li_xSO_y species were detectable. The overcharging capacity could be explained as a reversible part and an irreversible part. The reversible capacity was from the sulfur active material oxidized to long-chain lithium polysulfide and elemental sulfur, and the irreversible capacity was from the long-chain lithium polysulfide oxidized to Li_xSO_y species. $LiNO_3$ was an effective additive of Li–S cells to prevent shuttle phenomenon, but the oxidation mechanism in $LiNO_3$ electrolyte system was different from the systems with active shuttle phenomenon. The $LiNO_3$ could react with Li_2S_n to form Li_xSO_y species. And the consumption of $LiNO_3$ reflected the negative effects of $LiNO_3$ on the irreversible oxidation of sulfur active material, which should be paid more attention.

References

[1] P.G. Bruce, S.A. Freunberger, L.J. Hardwick, J.M. Tarascon, Nat. Mater. 11 (2012) 19.
[2] X. Ji, L.F. Nazar, J. Mater. Chem. 20 (2010) 9821.
[3] D. Aurbach, E. Pollak, R. Elazari, G. Salitra, J. Electrochem. Soc. 156 (2009) A694.
[4] V.S. Kolosnitsyn, E.V. Karaseva, Russ. J. Electrochem. 44 (2008) 506.
[5] Y.V. Mikhaylik, J.R. Akridge, J. Electrochem. Soc. 151 (2004) A1969.
[6] Y. Mikhaylik, I. Kovalev, R. Schock, K. Kumaresan, J. Xu, J. Affinito, ECS Trans. 35 (2010) 23.
[7] Y. Diao, K. Xie, S. Xiong, X. Hong, J. Electrochem. Soc. 159 (2012) A421.
[8] S.E. Cheon, K.S. Ko, J.H. Cho, S.W. Kim, E.Y. Chin, J. Electrochem. Soc. 150 (2003) A796.
[9] S.E. Cheon, S.S. Choi, J.S. Han, Y.S. Choi, B.H. Jung, H.S. Lima, J. Electrochem. Soc. 151 (2004) A2067.
[10] S.E. Cheon, K.S. Ko, J.H. Cho, S.W. Kim, E.Y. Chin, J. Electrochem. Soc. 150 (2003) A800.
[11] Y. Diao, K. Xie, S. Xiong, X. Hong, J. Electrochem. Soc. 159 (2012) A1816.
[12] D. Aurbach, O. Chusid, J. Power Sources 68 (1997) 463.
[13] D. Aurbach, O. Chusid, J. Electrochem. Soc. 140 (1993) L1.
[14] H. Ota, Y. Sakata, X. Wang, J. Sasahara, E. Yasukawa, J. Electrochem. Soc. 151 (2004) A437.
[15] C.D. Wagner, A.V. Naumkin, A. Kraut-Vass, J.W. Allison, C.J. Powell, J.R. Rumble, Nist X-ray Photoelectron Spectroscopy Database, NIST Standard Reference Database 20, Version 3.5 (2007).http://srdata.nist.gov/xps/.
[16] Y. Yang, G. Yu, J.J. Cha, H. Wu, M. Vosgueritchian, Y. Yao, Z. Bao, Y. Cui, ACS Nano 5 (2011) 9187.
[17] R.D. Cakan, M. Morcrette, F. Nouar, C. Davoisne, T. Devic, D. Gonbeau, R. Dominko, C. Serre, J.M. Tarascon, J. Am. Chem. Soc. 133 (2011) 16154.
[18] H. Sun, G.L. Xu, Y.F. Xu, S.G. Sun, X. Zhang, Y. Qiu, S. Yang, Nano Res. 10 (2012) 726.
[19] Y.X. Wang, L. Huang, L.C. Sun, S.Y. Xie, G.L. Xu, S.R. Chen, Y.F. Xu, J.T. Li, S.L. Chou, S.X. Dou, S.G. Sun, J. Mater. Chem. 22 (2012) 4744.
[20] F.F. Zhang, X.B. Zhang, Y.H. Dong, L.M. Wang, J. Mater. Chem. 22 (2012) 11452.
[21] S. Xiong, K. Xie, Y. Diao, X. Hong, Electrochim. Acta 83 (2012) 78.